Utah State University

DigitalCommons@USU

5-2012

Carrier Frequency Offset Estimation for Orthogonal Frequency Division Multiplexing

Nagaravind Challakere
Utah State University

Recommended Citation

CARRIER FREQUENCY OFFSET ESTIMATION FOR ORTHOGONAL

FREQUENCY DIVISION MULTIPLEXING

by

Nagaravind Challakere

A thesis submitted in partial fulfillment
of the requirements for the degree

of

MASTER OF SCIENCE

in

Electrical Engineering

Approved:

_____   _____
Dr. Jacob Gunther   Dr. Todd K Moon
Major Professor   Committee Member

_____   _____
Dr. Edmund Spencer   Dr. Mark R. McLellan
Committee Member   Vice President for Research and
                                         Dean of the School of Graduate Studies

UTAH STATE UNIVERSITY
Logan, Utah

2012

Abstract

Carrier Frequency Offset Estimation for Orthogonal Frequency Division Multiplexing

by

Nagaravind Challakere, Master of Science

Utah State University, 2012

Major Professor: Dr. Jacob Gunther
Department: Electrical and Computer Engineering

This thesis presents a novel method to solve the problem of estimating the carrier frequency offset in an Orthogonal Frequency Division Multiplexing (OFDM) system. The approach is based on the minimization of the probability of symbol error. Hence, this approach is called the Minimum Symbol Error Rate (MSER) approach. An existing approach based on Maximum Likelihood (ML) is chosen to benchmark the performance of the MSER-based algorithm. The MSER approach is computationally intensive. The thesis evaluates the approximations that can be made to the MSER-based objective function to make the computation tractable. A modified gradient function based on the MSER objective is developed which provides better performance characteristics than the ML-based estimator. The estimates produced by the MSER approach exhibit lower Mean Squared Error compared to the ML benchmark. The performance of MSER-based estimator is simulated with Quaternary Phase Shift Keying (QPSK) symbols, but the algorithm presented is applicable to all complex symbol constellations.

(51 pages)

Public Abstract

Carrier Frequency Offset Estimation for Orthogonal Frequency Division Multiplexing

by

Nagaravind Challakere, Master of Science

Utah State University, 2012

Major Professor: Dr. Jacob Gunther
Department: Electrical and Computer Engineering

The objective of the research for this thesis is to improve the performance of the Orthogonal Frequency Division Multiplexing (OFDM) system by minimising the impact of frequency offset at the receive end. OFDM is a popular standard used in wireless communication systems such as cellphone networks and broadband internet. In an OFDM system, the data symbols modulate the carrier signal at the transmitter. Usually, the receiver function generator performs the demodulation task. In the absence of frequency offset compensation, the transmitted symbols can not be effectively recovered upon reception. This leads to packet loss and a degradation of the Quality of Service (QoS) offered by the service provider.

Several approaches have been proposed to estimate the frequency offset at the receiver. Estimators based on Maximum Likelihood (ML) principle offer good system performance and are simple to implement. In this thesis an algorithm to estimate the frequency offsset is proposed. The objective of the algorithm is to minimise the probability of symbol error. The frequency estimate is chosen such that the probability of symbol error is minimised. The run-time performance of the system is improved as a part of the thesis.

Acknowledgments

I would like to express my highest regards and gratitude to my advisor, Dr. Jacob Gunther, without whose support this work would not have been possible. His constant guidance and motivation helped me gain the necessary skills in the fields of Digital Signal Processing and Communication Systems and inspired me to undertake this project. I would also like to thank Dr. Moon whose course on Mathematical Methods helped me attain the analytical skills necessary for my research. I must also thank Dr. Roger West who has been one of the biggest sources of inspiration for me as a student.

I would like to thank my father, C S Sathyanarayana Rao, who has always been both my staunchest supporter and my strongest critic. I would like to thank my sister, Anupama, for all her love. My eduacation at Utah would have not possible without the support of my sister, Nagashree, and my brother-in-law, Chaitanya Vishnu.

Finally, I would like to thank my dear friends: Sharath, Prasanna, Praveen, Yogi, Nithin, Nishant, Swathi, Nagi, Chandu, Karthik, Amritha, Thejas, Ravi Kant, Mangalam, Vipin, Purna, Kalyan, Sushant, Anitha, and members of "944" with whom I have spent some of the best times of my student life.

<div align="right">Nagaravind Challakere</div>

Contents

List of Figures

Chapter 1

Introduction

With the advent of personal communications, the demand for mobile and broadband wireless access has been ever increasing. The requirement for higher data rates has been met by the use of multicarrier techniques. Multicarrier techniques are particularly favored because of their robustness against frequency-selective fading encountered in mobile communications [1]. Frequency Division Multiplexing (FDM), Direct-Sequence Spread Spectrum (DSSS), and Orthogonal Frequency Division Multiplexing (OFDM) are some of the commonly employed techniques for multicarrier transmission. OFDM is favored in several communication standards because of the simplicity of its implementation and bandwidth efficiency. Fourth-generation (4G) systems, such as Mobile WiMAX and Long Term Evolution (LTE), favor the use of OFDM over DSSS which was the prominent choice in Third-generation (3G) systems such as Evolution-Data Optimized (EV-DO) and High-Speed Packet Access (HSPA). OFDM is an integral part of several wireless (IEEE 802.11a/g/n, DVB-T, and WiMAX) and wireline (ADSL and ITU-T G.hn) transmission protocols [2, 3].

1.1 Multicarrier Techniques

The basic idea of multicarrier transmission is to combat Intersymbol Interference (ISI) of a channel. If τ_m is the delay spread of a channel and T_s denotes the symbol duration then the transmission will be free of ISI if and only if the condition $\tau_m \ll T_s$ is met with $R_b = \log_2(M)T_s^{-1}$ being the maximum possible bit rate. In multicarrier transmission this limitation on maximum bit rate is overcome by splitting the data into K substreams of lower data rate and to transmit these substreams on adjacent subcarriers. The subcarrier bandwidth is now $\frac{B}{K}$, allowing for K times higher bit rate for a given value of delay spread.

This implementation with an FDM system is shown in figure 1.1.

The FDM system requires K separate RF modulators for transmission. The guard bands add to the bandwidth requirement of FDM, thus making it inefficient. These disadvantages can be overcome in OFDM by the use of orthogonal subcarriers to eliminate guard bands.

1.2   Overview of OFDM

OFDM is a bandwidth efficient multicarrier technique. The idea that orthogonal subcarriers can be used in multicarrier transmission was first proposed by R. W. Chang [4]. The requirement for guard bands is eliminated by the use of orthogonal subcarriers. Using the DFT to modulate the low rate data streams with orthogonal subcarriers was put forth by Weinstein and Ebert [5]. Figures 1.2 and 1.3 show the basic structure of the OFDM transmitter and receiver in IEEE 802.16e. The functionality of various subsystems will be revisited in section 2.1.

1.3   Impact of Frequency Offset

The spacing between adjacent subcarriers in an OFDM system is typically very small, and hence accurate frequency synchronization is very important. Carrier Frequency Offset (CFO) is introduced in the system due to local oscillator inaccuracies and Doppler Shift in the case of receiver motion. Due to the the residual frequency offset the orthogonality between transmit and receive pulses will be lost and the received symbols will have a time-variant phase rotation [6]. In figure 1.4 we see the effect of normalized residual frequency
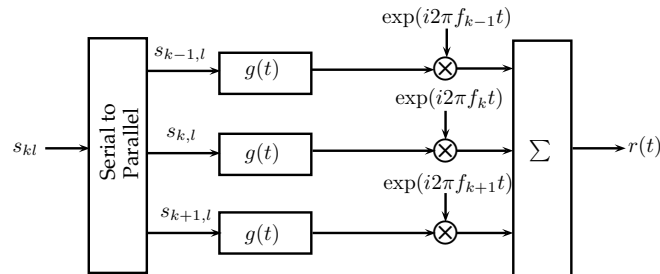
Fig. 1.1: Frequency division multiplexing system.
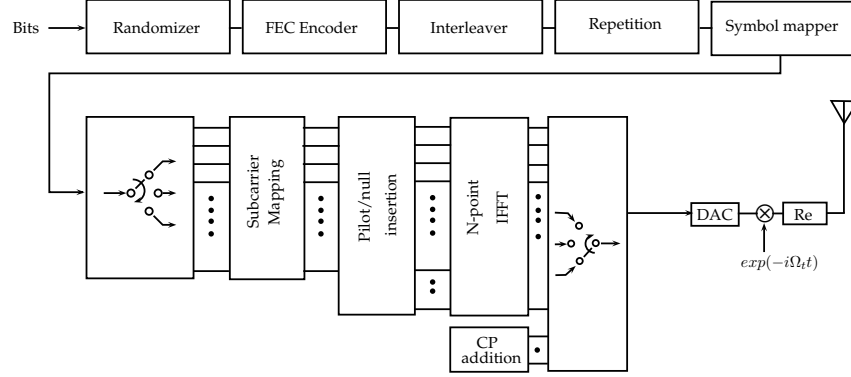
Fig. 1.2: OFDM transmitter in IEEE 802.16e.
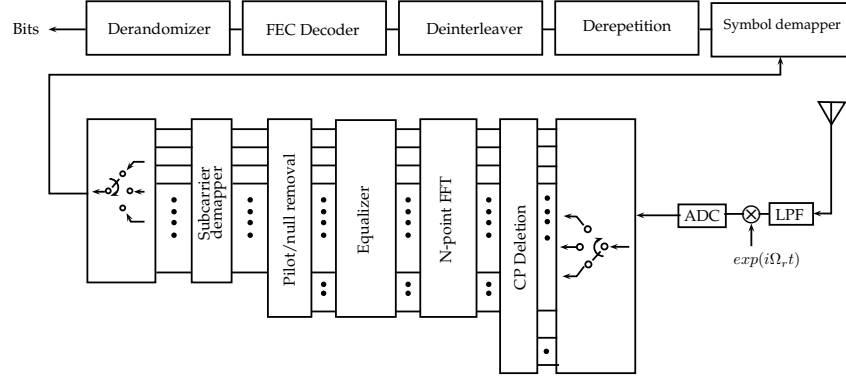
Fig. 1.3: OFDM receiver structure in IEEE 802.16e.

offsets of 0.05 and 0.1 on the received symbols at the zeroth subcarrier of 100 OFDM symbol blocks each with 256 subcarriers. The rotation of the constellation is due to the phase offset and the spreading of the symbols can be attributed to the presence of ICI. The addition of noise (AWGN) at the channel complicates the recovery even further. Figure 1.5 shows the same symbols with AWGN noise at 10 dB added in the channel.

1.4 Mitigating the Effects of CFO

Sathananthan and Tellambura [7] obtained analytical expressions for the computuation of probability of error due to CFO in OFDM systems in the presence of AWGN channel noise. With the increasing use of OFDM in most modern wireless and broadband access protocols CFO mitigation has been an active research domain. The approaches to mitigating the effects of CFO in OFDM tranceiver can be broadly classified into two categories.
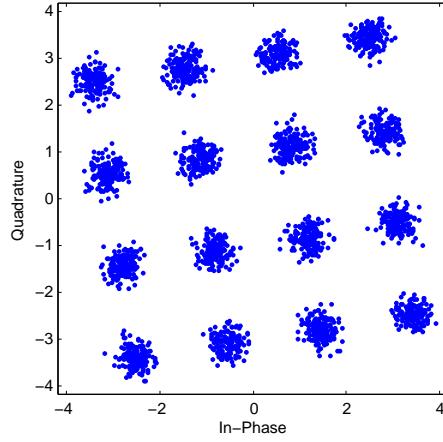
Fig. 1.4: Effect of normalized frequency offset = 0.05 on received symbols in a noiseless OFDM system.
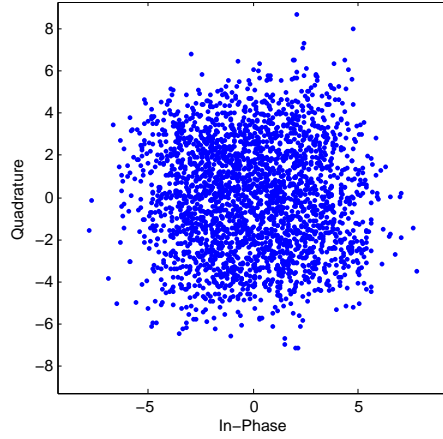
Fig. 1.5: Effect of normalized frequency offset = 0.05 on received symbols in the presence of noise with SNR = 10 dB.

In the first category the objective is to design the OFDM system, usually via subcarrier positioning, repetition of symbols and increasing block length using prefix data, such that even as CFO manifests in the system the symbols can be recovered. Several methods have been developed to reduce the effect of carrier frequency offset on OFDM. These approaches generally introduce analytical relationships between consecutive symbols to combat Inter-carrier Interference (ICI). Self-ICI cancellation schemes and windowing are some of the proposed approaches [8–10] to combat ICI. These approaches suffer from the disadvantage that they use a significant part of each OFDM block for ICI cancellation thereby reducing throughput.

The second approach is to estimate the value of the carrier frequency offset which can be used to recover the transmitted symbols. The major advantage of CFO estimation techniques is the increased throughput as the number of known symbols per block is reduced. CFO estimation strategies are evaluated based on the Mean Squared Error (MSE) of the CFO estimate and their performance in presence of a time-varying frequency offset. The attributes of the OFDM tranceiver structure can be used in estimating CFO. Liu and Tureli used polynomial root finding to estimate CFO in OFDM system with Cyclic Prefix (CP) [11]. The L subcarriers used for cyclic prefix are orthogonal to the N subcarriers that carry data symbols. In the presence of CFO the projection of the received vector onto the space of orthogonal subcarriers is nonzero. The CFO can be estimated by forcing the projection to zero. The method proposed by Liu and Tureli does not require the transmission of pilot symbols. Such methods belong to the class of blind estimation techniques. Roman et al. [12] propose a blind estimation technique using the cost function that minimizes the total off diagonal power induced by ICI in the received signal pseudo-correlation matrix. Tureli et al. have proposed an ESPRIT-like algorithm to estimate CFO from the correlation of received symbols [13]. Statistical functions of the equalized vector such as kurtosis have also been used in blind CFO estimation by Yao and Giannakis [14].

Blind techniques using a maximum likelihood (ML) cost function have been proposed for CFO estimation. These techniques usually rely on the symbol correlation to estimate the CFO. Symbol correlation in OFDM block using cyclic prefix was used in the estimation of CFO by van de Beek et al. [15]. This algorithm yields CFO estimate with low MSE and has the added advantage of low computational complexity.

Pilot symbols in transmitted OFDM block can be used in estimating the CFO. An ML estimation algorithm with the repeated use of a single data symbol was developed by Moose [16]. A rapid synchronisation method for CFO estimation with just two pilot symbols was developed by Schmidl and Cox [17]. Morelli and Mengali [18] extended upon this method by the use of multiple pilot symbols to obtain the CFO estimate with improved accuracy. Recent WLAN standards such as IEEE 802.11a allow for the use of four subcarriers

to carry pilot symbols within a block length of 48 symbols [19]. The use of null-subcarriers and their positioning in the OFDM block for CFO estimation is discussed by Ghogho et al. [20].

Minimum Symbol Error Rate criterion developed as an alternative to traditional Minimum Mean Square Error (MMSE)-based equalization techniques. Adaptive Minimum Bit Error Rate (MBER) equalization was introduced by Yeh and Barry for binary modulation schemes [21]. An Adaptive Minimum Symbol Error Rate (MSER) algorithm was later proposed by them to include pulse amplitude modulation (PAM) and quadrature amplitude modulation (QAM) constellations [22]. The notion of minimizing the probability of error was extended to include Bayes Risk (BR) in the Adaptive Minimum Bit Error Rate (AMBER) Equalization algorithm developed by Gunther and Moon [23].

1.5   Overview of Thesis

In this thesis, the MSER criterion will be used to estimate and compensate for carrier frequency offset at the receiver. The organization of the thesis is as follows. Chapter 2 provides an introduction to the OFDM data model used in the thesis and the development of expressions for the probability of error and its derivative. It also provides a discussion of the ML-based algorithm for CFO estimation from the approach proposed by van de Beek et al. [15]. Chapter 3 presents the implementation of the MSER-based CFO estimator followed by a discussion on the performance of the estimator. The estimator performance is contrasted vis-a-vis the ML-based CFO estimator particularly with respect to the MSE and BER. Chapter 4 presents the conclusion of the thesis with a discussion on the relative merits of the algorithms and defines the scope of future work to be done on this topic.

Chapter 2

CFO Estimation

This chapter discusses the development of an algorithm to estimate CFO in an OFDM system and forms the crux of this thesis. The first section of the chapter, derives the equations for the received symbol vector in the presence of noise and Carrier Frequency Offset (CFO). Section 2.2 defines a function that provides a measure of the impact of CFO on the average probability of error in the received symbols. The nature of such an error function provides the means to identify the magnitude of CFO based on observed symbols. In the subsequent sections, observations are made about the analytical nature of such an error function and how it improves the performance of the estimation algorithm.

2.1 Data Model

Chapter 1 (Figures 1.2 and 1.3), discussed the implementation of an OFDM transmitter based on IEEE 802.16e standard. While that diagram illustrates the components that would make up the OFDM transmitter, in formulating a model to reduce Carrier Frequency Offset it would be reasonable to eliminate the components that do not necessarily affect the estimation of the CFO. The *randomizer* eliminates long runs of 0s and 1s, in addition to adding to the security of the system by making the coded bitstream unintelligible to eavesdroppers. In an analysis of the impact of CFO on the demodulation of the received bits it may be safely assumed that the received bits are time-synchronised with the receiver clock.

The IEEE 802.16e standard mandates the use of a Convolutional code, denoted as FEC functions in Figures 1.2 and 1.3. It is interesting to couple the performance of an MSER-based CFO Estimator that utilises the noise immunity offered by block turbo codes, but the analysis of the MSER algorithm coupled with convolutional codes is beyond the

scope of this thesis. The *interleaver* and *subcarrier mapper* ensure that the encoded bits are separated in frequency space and constellation space. While these are practical considerations in the implementation of the OFDM tranceiver, they may be omitted from this discussion without loss of relevance. For the purposes of this section, and throughout this work, we will assume that the conversion between Analog and Digital formats is lossless (i.e., the ADCs and DACs are ideal).

Under these assumptions, the reference OFDM tranceiver can operate entirely in the digital domain and is shown in figures 2.1 and 2.2.

2.1.1 Expressions for Transmitted and Received Symbols

Let $\mathbf{s} = [s_1, s_2, \ldots s_N]^T$ be the vector of symbols from the complex alphabet $\mathcal{A} = \{a_1, a_2, \ldots a_M\}$ that have been mapped from the input bit vector $\mathbf{b}$. Let $\mathbf{t}$ denote the output of the IFFT block. Using the matrix notation W to denote the inverse Fourier Transform we have

$$\mathbf{t} = \mathrm{W}\mathbf{s}. \tag{2.1}$$

The subcarrier modulated symbol vector $\mathbf{t}$ is used to modulate the carrier signal at frequency f_t. This operation can be denoted using the vector notation as

$$\mathbf{u} = \mathrm{F}_t\mathbf{t}$$
$$= \mathrm{F}_t\mathrm{W}\mathbf{s}, \tag{2.2}$$
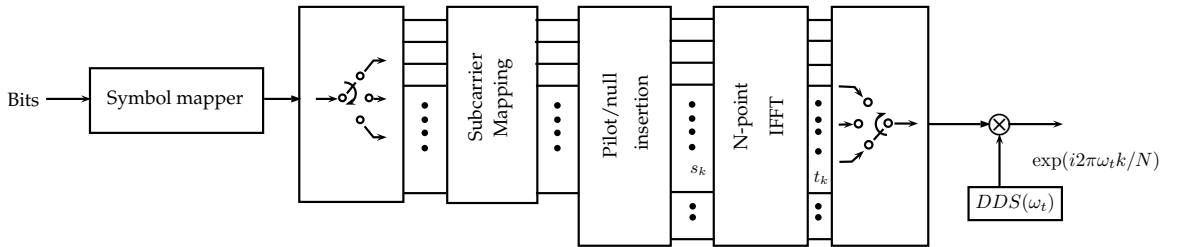
Fig. 2.1: OFDM transmitter - Modified to suit discussion about CFO estimation.
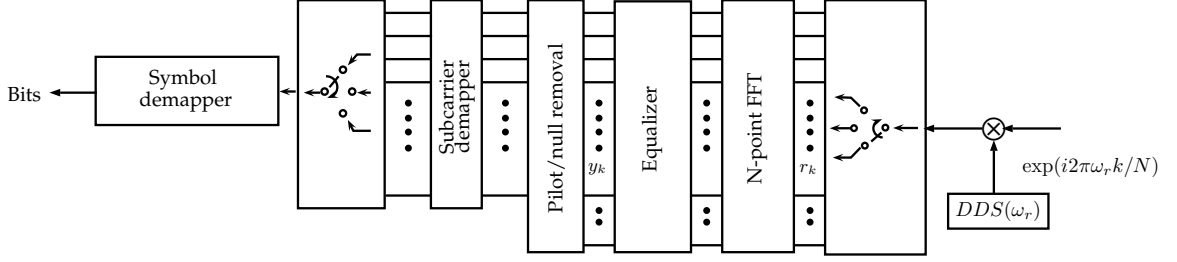
Fig. 2.2: Simplified OFDM receiver designed to complement functionality of the OFDM transmitter.

where $F_t = \text{diag}(1, \exp(i\omega_t/N), \exp(i2\omega_t/N) \ldots \exp(i(N-1)\omega_t/N))$ denotes the modulation by the transmitter-side Direct Digital Synthesizer (DDS) and $\omega_t = 2\pi f_t$ is the frequency of the transmit DDS.

In the presence of channel noise, the received symbol vector $\mathbf{r}$ can be represented as

$$\mathbf{r} = \mathbf{u} + \mathbf{z}$$

$$= F_t W \mathbf{s} + \mathbf{z}, \tag{2.3}$$

where $\mathbf{z}$ denotes the complex circular white Gaussian noise added by the channel. At the receiver, demodulation consists of translating the received signal to baseband frequency followed by taking the DFT of the resultant signal. Let $\omega_r = 2\pi f_r$ be the receiver DDS frequency.

The equalizer output $\mathbf{y}$ can thus be represented as

$$\mathbf{y} = \text{FFT}\{F_r^H \mathbf{r}\}$$

$$= W^H F_r^H (F_t W \mathbf{s} + \mathbf{z})$$

$$= W^H F_r^H F_t W \mathbf{s} + W^H F_r^H \mathbf{z}, \tag{2.4}$$

where $F_r = \text{diag}(1, \exp(i\omega_r/N), \exp(i2\omega_r/N) \ldots \exp(i(N-1)\omega_r/N))$ denotes the modulation by the receiver DDS. In the absence of CFO, the receiver DDS frequency $\omega_r = \omega_t$ and the equalizer ouputs are the transmitted constellation symbols in the presence of Gaussian noise. The random vector $\mathbf{z}$ denotes a complex circular white Gaussian random vector, and

hence multiplication by the unitary matrices W^H and F_R does not alter this property. Let $\eta = W^H F_r^H z$ denote the noise component. Also, let $P = F_r^H F_t$ denote the uncompensated CFO matrix. Thus,

$$\begin{aligned} y &= W^H F_r^H F_t W s + W^H F_r^H z \\ &= W^H P W s + \eta. \end{aligned} \tag{2.5}$$

Since, W and P are unitary matrices $\eta \in \mathbb{C}^N$ is a circular complex Gaussian random vector. Let $\sigma^2 I$ be the covariance matrix of η.

Denoting $W^H P W$ as H,

$$y = Hs + \eta. \tag{2.6}$$

The demodulated symbol y_i at the ith subcarrier is given by

$$y_i = \mathbf{h}_i^T s + \eta_i, \tag{2.7}$$

where $\mathbf{h_i}^T$ denotes the ith row of the matrix H.

Further, $y \in \mathbb{C}^N$. Let us define a mapping rule $\mathcal{D} : \mathbb{C} \mapsto \mathcal{A}$ and $\hat{y}_n = \mathcal{D}(y_n)$ be the decision on y_n. The error event for the nth symbol is thus,

$$e_n := \{\hat{y}_n \neq s_n\}. \tag{2.8}$$

The objective of the carrier frequency offset estimator is to minimize the error in mapping the decoded symbol $\hat{y}_n$, under operating conditions defined by the noise variance σ^2 and the frequency offset ν.

2.1.2 Note on Carrier Frequency Offset

As mentioned earlier, the digital frequencies ω_t and ω_r denote the transmitter and receiver DDS frequencies. The following relations apply between the digital frequencies in

figures 2.1 and 2.2 and the analog frequencies Ω_t and Ω_r in figures 1.2 and 1.3.

$$\omega_t = \Omega_t \times T_s \tag{2.9}$$

$$\omega_r = \Omega_r \times T_s \tag{2.10}$$

$$\nu = \frac{1}{2\pi}(\omega_t - \omega_r) \tag{2.11}$$

$$= \frac{1}{2\pi}(\Omega_t - \Omega_r) \times T_s. \tag{2.12}$$

As per the Nyquist criterion, the bandwidth required for N orthogonal pulses is $B = \frac{N}{2T_s}$. The Carrier Frequency Offset (CFO) can thus be expressed as

$$\nu = \frac{1}{2\pi}(\Omega_t - \Omega_r) \times \frac{N}{2B}. \tag{2.13}$$

2.2 Probability of Error under MSER Criterion

In this section, a general expression for the average probability of symbol error is derived under the MSER criterion. The notations used in this section will be particularly relevant in the subsequent sections where the OFDM data model will be considered. For this discussion, we will assume a vector of transmitted data symbols $\mathbf{s} = [s_1, s_2, \ldots s_N]$ where each $s_i \in \mathcal{A}$. Let $\mathbf{y}, y_n, \mathcal{D} : \mathbb{C} \mapsto \mathcal{A}$ denote the output of the equalizer at the receive end, equalizer output at n^{th} symbol duration and the decision rule to classify symbols, respectively. While discussing the data model in section 2.1.1, we defined $\mathcal{A}$ to be the constellation of complex symbols which are to be recovered at the OFDM receiver. In the traditional approach to classify a recovered symbol $y \in \mathbb{C}$ the decision rule divides the constellation $\mathcal{A}$ into disjoint regions $\mathcal{R}_i, i = 1, 2, \ldots, M$ in which the individual regions are given by

$$\mathcal{R}_i = \{y : |y - a_i| < |y - a_k| \;\; \forall k \neq i\}. \tag{2.14}$$

Thus if the transmitted symbol s_n is known to be a_i, the error event in (2.8) can be expressed as

$$e_n = \{\hat{y}_n \neq s_n\}$$
$$= \{y_n \notin \mathcal{R}_i\}. \tag{2.15}$$

Lemma 2.1. *The probability of error for a symbol in the nth location, which will be denoted as $P(e_n)$, can be expressed as*

$$P(e_n) = E_{s_n = a_i} E_{\mathbf{s}[a_i]} P(y_n \notin \mathcal{R}_i | \mathbf{s}[a_i]). \tag{2.16}$$

Proof. The probability of the considered symbol being in error is an implicit function in terms of the transmitted symbols, the magnitudes of additive noise and the frequency offset. From (2.8),

$$P(e_n) = P(\hat{y}_n \neq s_n).$$

The probability of error can be expressed as the piecewise sum conditioned on the probabilty of occurence of the individual symbols, i.e.

$$P(e_n) = \sum_{i=1}^{M} P(\hat{y}_n \neq s_n | s_n = a_i) P(s_n = a_i), \tag{2.17}$$

$$P(e_n) = \frac{1}{M} \sum_{i=1}^{M} P(\hat{y}_n \neq s_n | s_n = a_i), \tag{2.18}$$

assuming all symbols are equally likely. If the probability of symbol error can be expressed as the marginal probability mass function by accounting for all possible combinations of the

symbol vector $\mathbf{s}$,

$$P(e_n) = \frac{1}{M} \sum_{i=1}^{M} \sum_{\mathbf{s}} P(\hat{y}_n \neq s_n, \mathbf{s} | s_n = a_i) \tag{2.19}$$

$$= \frac{1}{M} \sum_{i=1}^{M} \sum_{\mathbf{s}} P(\hat{y}_n \neq s_n | \mathbf{s}, s_n = a_i) P(\mathbf{s} | s_n = a_i). \tag{2.20}$$

Here the law of conditional probability $P(A, B|C) = P(A|B, C)P(B|C)$ and the notation $E[g(X)] = \sum_{x_i} g(x_i) P(X = x_i)$ for the expected value of a random variable have been used.

$$P(e_n) = \frac{1}{M} \sum_{i=1}^{M} E_{\mathbf{s}|s_n=a_i} P(\hat{y}_n \neq s_n | \mathbf{s}, s_n = a_i) \tag{2.21}$$

Since $\mathbf{s}|s_n = a_i$ implies the symbol vector $\mathbf{s} = [s_1, \ldots, s_{n-1}, a_i, s_{n+1}, \ldots s_N]$, we can denote it as $\mathbf{s}[a_i]$, as is the event $\{\mathbf{s}, s = a_i\}$.

$$\therefore P(e_n) = \frac{1}{M} \sum_{i=1}^{M} E_{\mathbf{s}[a_i]} P(\hat{y}_n \neq s_n | \mathbf{s}[a_i]) \tag{2.22}$$

Substituting (2.15) in (2.22) and expressing the sum over symbol probabilities as an expectation,[1]

$$P(e_n) = E_{s_n=a_i} E_{\mathbf{s}[a_i]} P(y_n \notin \mathcal{R}_i | \mathbf{s}[a_i]). \tag{2.23}$$

2.2.1   Alternative Decision Rule for Categorising Symbol Error

Decision regions $\mathcal{S}_i$ and $\mathcal{S}_k$ can be defined for every pair of symbols a_i and a_k such that

$$\mathcal{S}_i = \{y : |y - a_i| < |y - a_k|\},$$

$$\mathcal{S}_k = \{y : |y - a_k| < |y - a_i|\}. \tag{2.24}$$

---

[1] Even though it is customary to express the expectation as E_{s_n}, $E_{s_n=a_i}$ is used for notational clarity.

These decision regions are shown for the case of 16-QAM as shown in figure 2.3.

Lemma 2.2. *For the case of the decision regions defined in section 2.2.1,*

$$P(y_n \in \mathcal{R}_i) \leq P(y_n \in \mathcal{S}_i). \tag{2.25}$$

Proof. The proof is based on $\mathcal{R}_i \subseteq \mathcal{S}_i$ which follows from the definitions of the regions in (2.14) and (2.24). Gunther and Moon [23] further note that equality is achieved in when $\mathcal{A}$ consists of just two points. Furthermore, equality is approximately achieved when a_i and a_k are neighbors in a large constellation and the signal-to-noise ratio is high.

2.2.2 Expression for Probability of Error

From (2.23) we have

$$P(e_n) = E_{s_n=a_i} E_{\mathbf{s}[a_i]} P(y_n \notin \mathcal{R}_i | \mathbf{s}[a_i])$$

$$= E_{s_n=a_i} E_{\mathbf{s}[a_i]} \sum_{\substack{k=1 \\ k \neq i}}^{M} P(y_n \in \mathcal{R}_k | \mathbf{s}[a_i]) \tag{2.26}$$

$$\leq E_{s_n=a_i} E_{\mathbf{s}[a_i]} \sum_{\substack{k=1 \\ k \neq i}}^{M} P(y_n \in \mathcal{S}_k | \mathbf{s}[a_i]) \tag{2.27}$$

$$= E_{s_n=a_i} E_{\mathbf{s}[a_i]} \sum_{k=1}^{M} I(k \neq i) P(y_n \in \mathcal{S}_k | \mathbf{s}[a_i]) \tag{2.28}$$

$$= E_{s_n=a_i} E_{\mathbf{s}[a_i]} \sum_{k=1}^{M} I(k \neq i) I(y_n \in \mathcal{S}_k) P(y_n | \mathbf{s}[a_i]). \tag{2.29}$$

The expectation over all possible equalizer output values can be completed to obtain the probability of error as

$$P(e) = E_{s_n=a_i} E_{\mathbf{s}[a_i]} E_{y_n | \mathbf{s}[a_i]} \sum_{k=1}^{M} I(k \neq i) I(y_n \in \mathcal{S}_k). \tag{2.30}$$
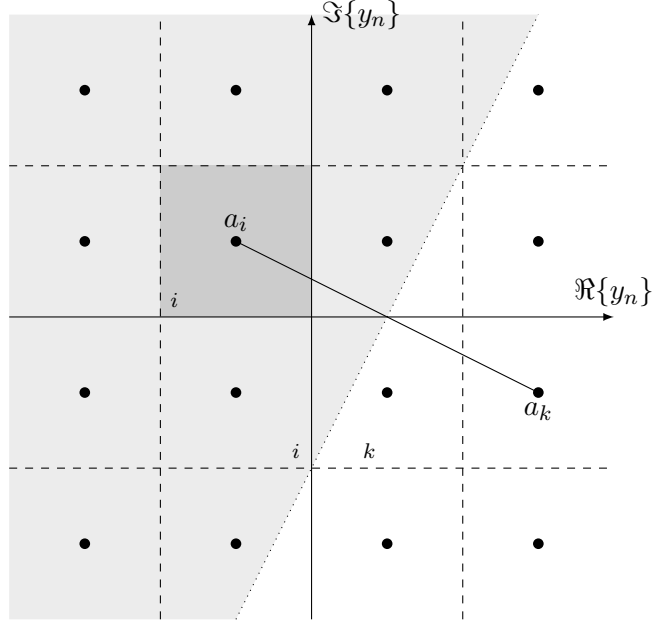
Fig. 2.3: Decision regions $\mathcal{S}_i, \mathcal{S}_k$ and $\mathcal{R}_i, \mathcal{R}_k$ for the case of 16-QAM.

2.3 Probability of Error for the OFDM Data Model

In this section, we will simplify the expression $P(y_n \in \mathcal{S}_k|\mathbf{s}[a_i])$ from (2.28). Considering (2.28), it can be seen that the conditional probability of error in the nth subcarrier can be expressed in terms of the probability that the equalizer output for the subcarrier lies in a different decision region than the transmitted symbol a_i, i.e.

$$y_n \in \mathcal{S}_k\big|\mathbf{s}[a_i] \iff |y_n - a_k|^2 < |y_n - a_i|^2|\mathbf{s}[a_i]. \tag{2.31}$$

The event $|y_n - a_k|^2 < |y_n - a_i|^2|\mathbf{s}[a_i]$ can be simplified as

$$\left\{ |y_n - a_k|^2 < |y_n - a_i|^2 \Big| \mathbf{s}[a_i] \right\}$$

$$\tag{2.32}$$

$$\implies \left\{ y_n^*(a_i - a_k) + (a_i - a_k)^* y_n < \frac{(a_i + a_k)^*(a_i - a_k)}{2} + \frac{(a_i - a_k)^*(a_i + a_k)}{2} \Big| \mathbf{s}[a_i] \right\}$$

$$\implies \left\{ (a_i - a_k)^*(y_n - \frac{a_i + a_k}{2}) + (y_n - \frac{a_i + a_k}{2})^*(a_i - a_k) < 0 \Big| \mathbf{s}[a_i] \right\}$$

$$\implies \left\{ 2 \times \Re((a_i - a_k)^*(y_n - \frac{a_i + a_k}{2})) < 0 \Big| \mathbf{s}[a_i] \right\}. \tag{2.33}$$

Substituting for y_n from (2.7),

$$\left\{ 2 \times \Re((a_i - a_k)^*(\mathbf{h_n}^T \mathbf{s} + \eta_n - \frac{a_i + a_k}{2})) < 0 \Big| \mathbf{s}[a_i] \right\}.$$

Observing that $\{\mathbf{h_n}^T \mathbf{s} \,|\mathbf{s}[a_i]\} = \mathbf{h_n}^T \mathbf{s}[a_i]$,

$$y_n \in \mathcal{S}_k \big| \mathbf{s}[a_i] \implies \Re((a_i - a_k)^*(\mathbf{h_n}^T \mathbf{s}[a_i] - \frac{a_i + a_k}{2})) < \Re(-(a_i - a_k)^* \eta_n) \tag{2.34}$$

$$P(y_n \in \mathcal{S}_k \big| \mathbf{s}[a_i]) = P\left(\Re((a_i - a_k)^*(\mathbf{h_n}^T \mathbf{s}[a_i] - \frac{a_i + a_k}{2})) < \Re(-(a_i - a_k)^* \eta_n) \right). \tag{2.35}$$

If η_n is zero-mean, circular, complex Gaussian noise with variance σ^2, then $(a_k - a_i)^* \eta_n \sim \mathcal{N}(0, |a_k - a_i|^2 \sigma^2)$ and $\Re((a_k - a_i)^* \eta_n) \sim \mathcal{N}(0, \frac{|a_k - a_i|^2}{2}\sigma^2)$.

$$P(\Re((a_k - a_i)^* \eta_n) > x) = Q\left(\frac{x}{\sqrt{\text{var}(\Re((a_k - a_i)^* \eta_n))}} \right) \tag{2.36}$$

Substituting (2.36) in (2.35) we get

$$P(y_n \in \mathcal{S}_k \big| \mathbf{s}[a_i]) = Q\left(\frac{\sqrt{2}\Re((a_i - a_k)^*(\mathbf{h_n}^T \mathbf{s}[a_i] - \frac{a_i + a_k}{2}))}{|a_k - a_i|\sigma} \right) \tag{2.37}$$

$$P(e_n | \mathbf{s}[a_i]) = \sum_{k=0}^{M-1} I(k \neq i) Q\left(\frac{\sqrt{2}\Re((a_i - a_k)^*(\mathbf{h_n}^T \mathbf{s}[a_i] - \frac{a_i + a_k}{2}))}{|a_k - a_i|\sigma} \right). \tag{2.38}$$

The probability of error for the OFDM data model can thus be expressed as

$$P(e) = E_{s_n = a_i} E_{\mathbf{s}[a_i]} E_{y_n | \mathbf{s}[a_i]} \sum_{k=0}^{M-1} I(k \neq i) Q\left(\frac{\sqrt{2}\Re((a_i - a_k)^*(\mathbf{h_n}^T \mathbf{s}[a_i] - \frac{a_i + a_k}{2}))}{|a_k - a_i|\sigma} \right). \tag{2.39}$$

2.4   Derivative of Probability of Error

This section develops an expression for the derivative of the probability of error for the OFDM data model. As mentioned earlier, the probability of error is implicitly a function of the carrier frequency offset. Taking the derivative of probability of error with respect to the CFO ν

$$\frac{\partial}{\partial\nu}P(e) = \frac{\partial}{\partial\nu}E_{s_n=a_i}E_{\mathbf{s}[a_i]}E_{y_n|\mathbf{s}[a_i]}\sum_{k=0}^{M-1}I(k \neq i)Q\left(\frac{\sqrt{2}\Re((a_i-a_k)^*(\mathbf{h_n}^T\mathbf{s}[a_i]-\frac{a_i+a_k}{2}))}{|a_k-a_i|\sigma}\right) \quad (2.40)$$

$$= E_{s_n=a_i}E_{\mathbf{s}[a_i]}E_{y_n|\mathbf{s}[a_i]}\sum_{k=0}^{M-1}I(k \neq i)\frac{\partial}{\partial\nu}Q\left(\frac{\sqrt{2}\Re((a_i-a_k)^*(\mathbf{h_n}^T\mathbf{s}[a_i]-\frac{a_i+a_k}{2}))}{|a_k-a_i|\sigma}\right). \quad (2.41)$$

Lemma 2.3. *The derivative of the Q-function with respect to ν is given by*

$$\frac{\partial}{\partial\nu}Q\left(\frac{\sqrt{2}\Re((a_i-a_k)^*(\mathbf{h}_n^T\mathbf{s}[a_i]-\frac{a_i+a_k}{2}))}{|a_k-a_i|\sigma}\right) = -Q\left(\frac{\sqrt{2}\Re((a_i-a_k)^*(\mathbf{h_n}^T\mathbf{s}[a_i]-\frac{a_i+a_k}{2}))}{|a_k-a_i|\sigma}\right)$$

$$\times \frac{\sqrt{2}\Re((a_i-a_k)^*(\dot{\mathbf{h}}_n^T\mathbf{s}[a_i]))}{|a_k-a_i|\sigma}. \quad (2.42)$$

Proof. See Appendix A.

2.5   ML Estimation of CFO

In Chapter 1, various proposed approaches to estimate CFO in OFDM systems were explained. The ML approach put forth by van de Beek et al. [15] is used to compare the performance of MSER approach. Even though it is a blind estimation technique, this approach yields CFO estimate with a low mean squared error along with a low BER for the system, and thus can be a good benchmark against which the performance of MSER can be measured. Given an OFDM block of length $N + L$ where N is the number of subcarriers for data and L is the length of the cyclic prefix, the ML estimate for the frequency offset in the received baseband signal $\mathbf{r}$ is given by

$$\hat{\nu}_{ML} = -\frac{1}{2\pi}\angle\sum_{k=1}^{L}r(k)r^*(k+N). \quad (2.43)$$

Chapter 3

Implementation and Results

In this section, we will obtain the results of simulating an OFDM system. The system model presented in figures 2.1 and 2.2 will be used with $N = 256$. For these simulations, it is assumed that all the symbols are known a-priori and are taken from the QPSK constellation. The simulation was carried out on the same OFDM block with the noise vector being averaged out with approximately 100 trials.

3.1 Approximations to Probability of Error using MSER

Under MSER criterion we obtained the following expressions for the probability of error and its derivative.

$$P(e) = E_{s_n=a_i} E_{\mathbf{s}[a_i]} E_{y_n|\mathbf{s}[a_i]} \sum_{k=0}^{M-1} I(k \neq i) Q\left(\frac{\sqrt{2}\Re((a_i-a_k)^*(\mathbf{h}_n^T\mathbf{s}[a_i]-\frac{a_i+a_k}{2}))}{|a_k-a_i|\sigma} \right) \quad (3.1)$$

$$\frac{\partial}{\partial \nu} P(e) = -E_{s_n=a_i} E_{\mathbf{s}[a_i]} E_{y_n|\mathbf{s}[a_i]} \sum_{k=0}^{M-1} I(k \neq i) Q\left(\frac{\sqrt{2}\Re((a_i-a_k)^*(\mathbf{h}_n^T\mathbf{s}[a_i]-\frac{a_i+a_k}{2}))}{|a_k-a_i|\sigma} \right)$$
$$\times \frac{\sqrt{2}\Re((a_i-a_k)^*(\dot{\mathbf{h}}_n^T\mathbf{s}[a_i]))}{|a_k-a_i|\sigma} \quad (3.2)$$

In the absence of knowledge of the CFO matrix H, the term $\mathbf{h_n}^T\mathbf{s}[a_i]$ can be replaced by its noisy estimate y_n. The expectation $E_{\mathbf{s}[a_i]} E_{y_n|\mathbf{s}[a_i]} = E_{y_n,\mathbf{s}[a_i]}$ is computationally intensive. An iterative algorithm operating on multiple blocks can be thought of as averaging over the $\mathbf{s}[a_i]$ part of the joint expectation and the gradient in (3.2) can be computed as the sum over data symbols in each block. With these observations (3.2) can be computed as

$$\frac{\partial}{\partial \nu} P(e) = -E_{s_n=a_i} E_{y_n} \sum_{k=0}^{M-1} I(k \neq i) Q\left(\frac{\sqrt{2}\Re((a_i-a_k)^*(y_n-\frac{a_i+a_k}{2}))}{|a_k-a_i|\sigma} \right)$$
$$\times \frac{\sqrt{2}\Re((a_i-a_k)^*(y_n))}{|a_k-a_i|\sigma}. \quad (3.3)$$

If the OFDM block length is sufficiently large and at higher values of SNR this estimate effectively approximates the actual expectation. It may be noted that in (3.3) the data symbols a_i are assumed to be known. This is generally true of OFDM systems in which it is customary to include Pilot symbols[1]. Alternatively a decision aided estimator can also be obtained with $\mathcal{D}\{y_n\}$ used in place of a_i. For large constellations (e.g. 64-QAM) the sum over k can be replaced by considering l-nearest neighbors.

3.2   S-Curves

The probability of error is a function in terms of system parameters such as N-the number of subcarriers in the OFDM block, σ Signal-to-Noise ratio (SNR) at which the system operates. The derivative of probability of error is also an important criterion as it aids the choice of the algorithm with which we will perform the CFO estimation. If probability of error is used as the objective function with LMS adaptation rule then the gradient of the probability of error determines the rate of convergence of the algorithm. The average value of the gradient is called the S-curve and is defined as

$$g(\nu_e) \triangleq E \frac{\partial}{\partial \nu} P(e). \tag{3.4}$$

Using S-curves we can obtain quantitative information about the performance of the estimation system. Figures 3.1 and 3.2 show the probability of error and the S-Curve at 10 dB. A distinct feature of the MSER based decision rule is that at sufficiently high SNR the system will not compensate beyond a small residual offset as shown in figure 3.2.

Figures 3.3-3.7 show the objective function and the S-curve at SNRs of -16 dB, -8 dB, 0 dB, 8 dB, and at 16 dB. The operating regions of -16 dB and -8dB are not usually encountered but are provided here for the sake of completeness.

The following observations can be made about the S-curves.

1. When the SNR is low (less than 0 dB) and the CFO is high, corresponding to figures 3.3

---

[1] IEEE 802.11a specification provides for four subcarriers dedicated for carrying pilot symbols in a block length of 48 [19]. Li et al. [24] note that the preamble structure for IEEE802.11 standard allows for nine short OFDM symbols of length 16 and 2 long OFDM symbols of length 64 to be used as pilots
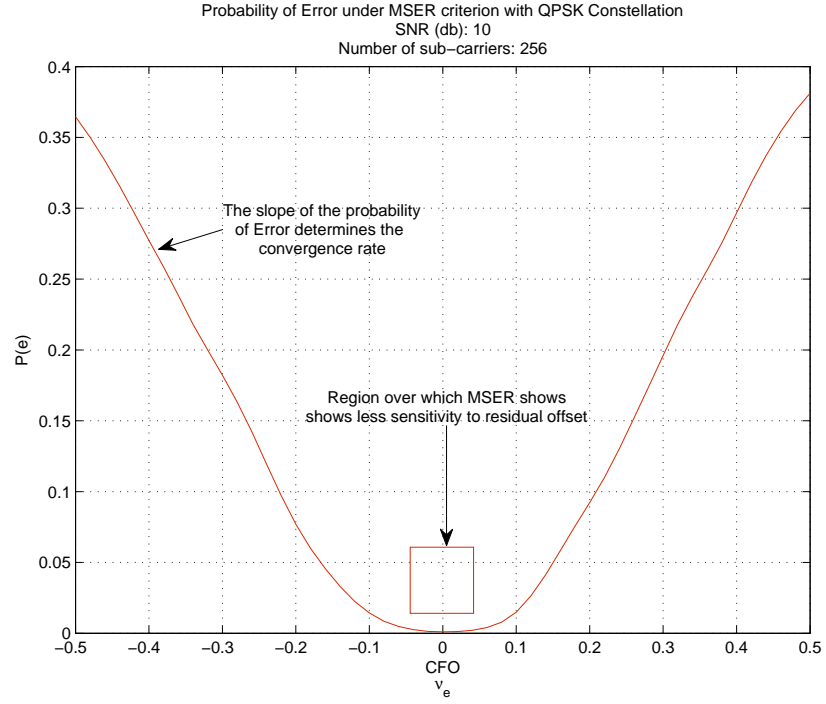
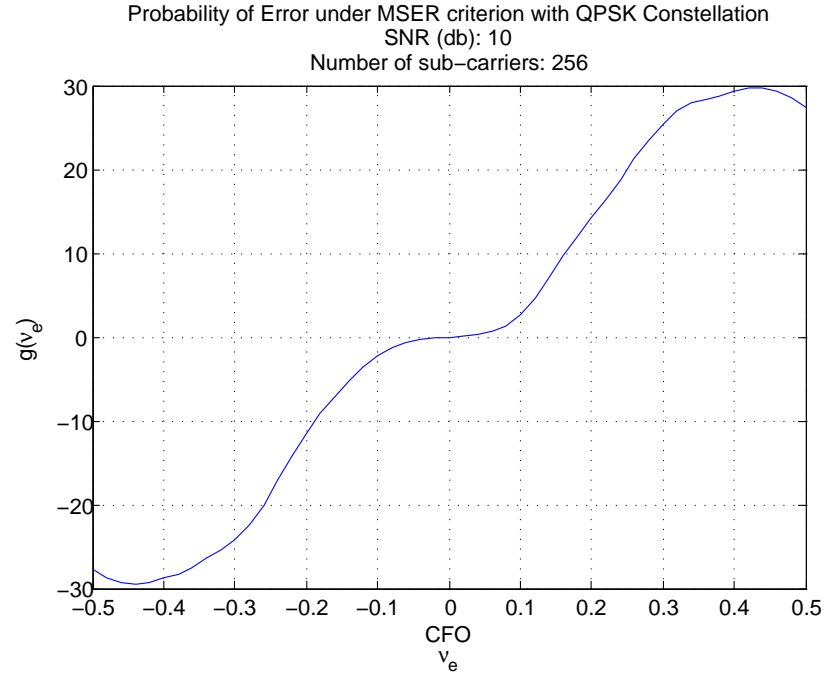Fig. 3.1: Probability of error as a function of uncompensated CFO at 10dB for QPSK constellation- N = 256.

Fig. 3.2: S-curve for OFDM system with QPSK contellation operating at 10dB- N = 256.

and 3.4, the S-curve passes through zero at $\nu_e = 0.2$ approximately. This corresponds to the residual offset of the system after convergence. The performance of the system is poorest in such conditions.

2. At moderate Signal-to-Noise ratios of operation, 0-8 dB corresponding to figures 3.5 and 3.6, the S-curve passes through the origin implying that the system converges to a zero residual offset. For the 8 dB case, the small gradient of the S-curve around zero suggests that the update to CFO estimate is very small once the system has converged the region of low probability of error. This implies that post-convergence the system has a low BER. This will be confirmed further in this section.

3. If the system operates at high SNR, 16 dB corresponding to figure 3.7, the behavior of the system around zero offset is similar to case 2. However, the slope of the S-curve beyond this point is much larger. This implies a large error signal at the beginning of adaptation. If an adaptive algorithm is to be implemented with MSER then the step size should be chosen to avoid the oscillation around the zero residual offset.

4. The range of frequencies at which the S-curve has a linear positive gradient denotes the acquisition range of the algorithm. Based on these S-curves we may conclude that MSER algorithm offers an acquisition range of approxiamtely $|\nu| \leq 0.5$.

3.3   MSER-Based CFO Estimator

In expression (3.3) $\dot{y}_n$ was used in computing the gradient of the error function. Figure 3.8 illustrates how $\dot{y}_n$ can be obtained given the received samples r_k and describes the structure of an estimator that updates the CFO estimate $\hat{\nu}$ once per OFDM block. CFO Estimator block performs the computuation of the error signal which is limited to the range $[-0.5, 0.5]$ at the mod-0.5 block to generate the CFO estimate for the next iteration using the LMS update equation

$$\hat{\nu}_{t+1} = \hat{\nu}_t - \delta_{MSER} g_{MSER}(\nu_e), \tag{3.5}$$

Fig. 3.3: Probability of error and S-curve for OFDM system with QPSK constellation operating at -16 dB.

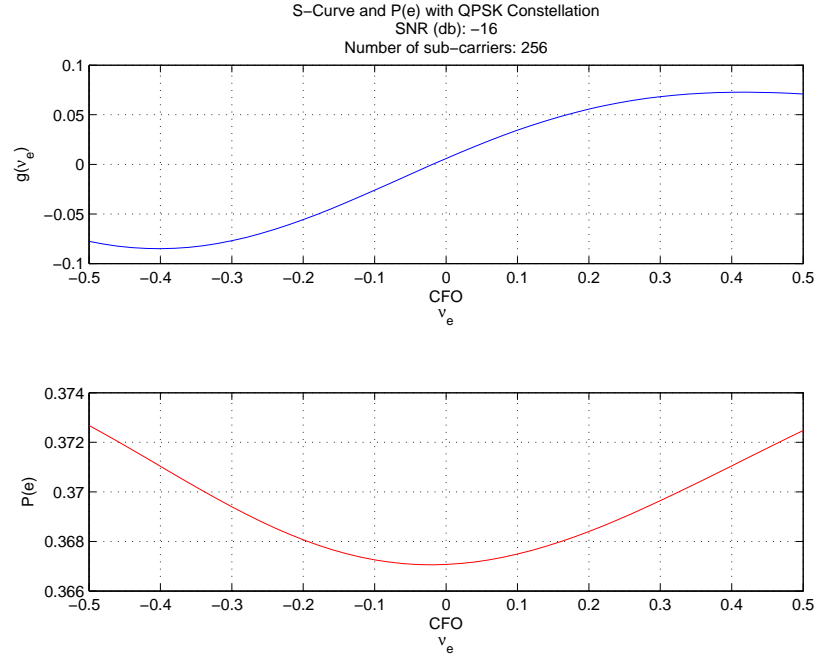Fig. 3.4: Probability of error and S-curve for OFDM system with QPSK constellation operating at -8 dB.

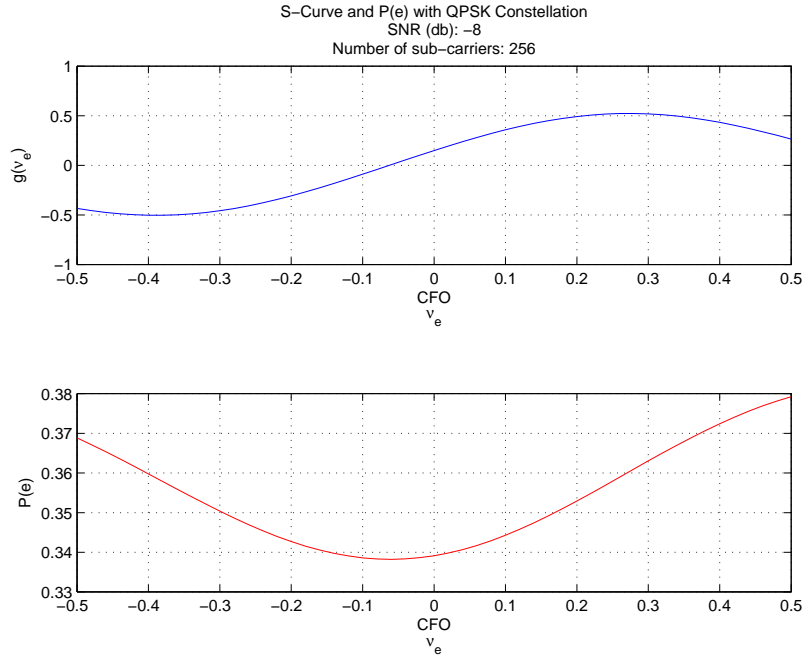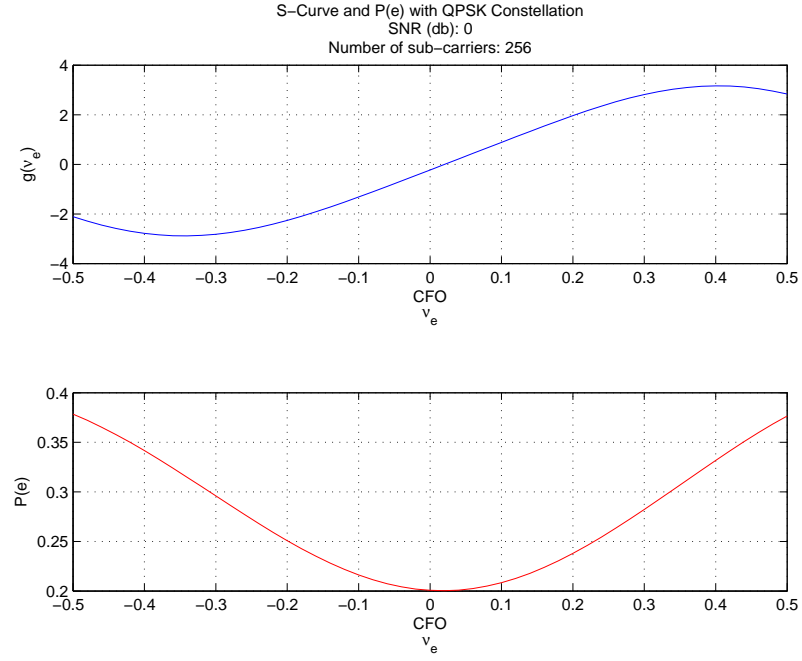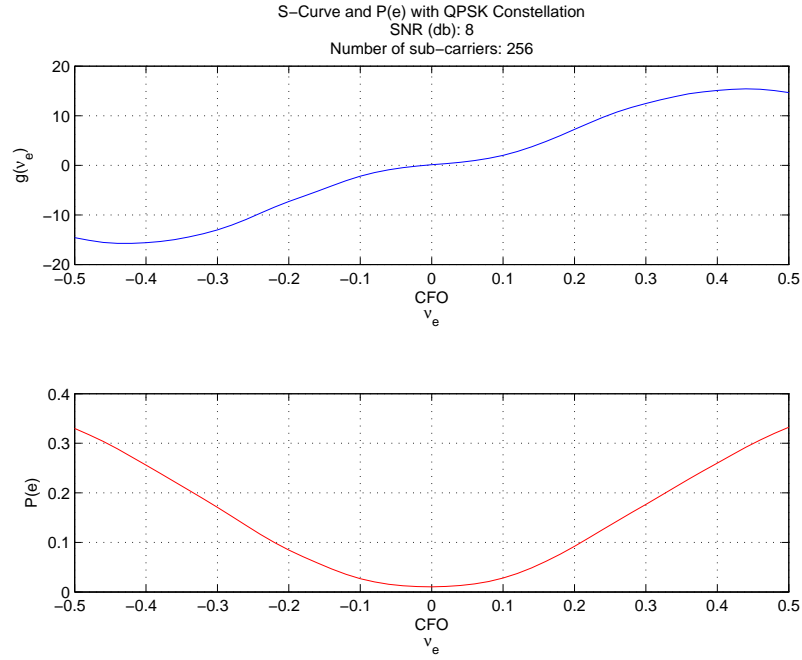Fig. 3.5: Probability of error and S-curve for OFDM system with QPSK constellation operating at 0 dB.

Fig. 3.6: Probability of error and S-curve for OFDM system with QPSK constellation operating at 8 dB.
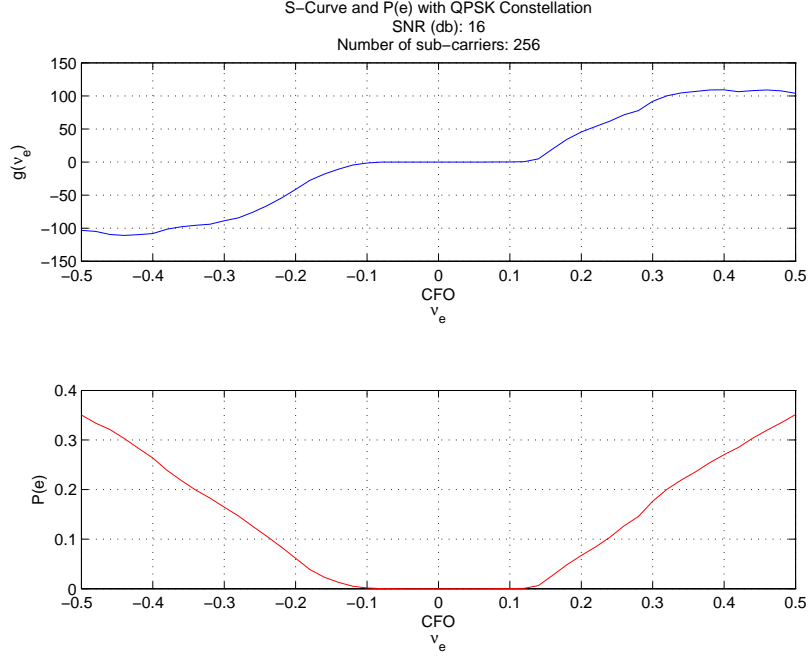
Fig. 3.7: Probability of error and S-curve for OFDM system with QPSK constellation operating at 16 dB.

where δ_{MSER} is the step-size of the update.

3.4 Results

In this section the results of simulating the OFDM system with MSER decision rule are discussed. QPSK constellation is used to generate data symbols. The OFDM block length, N, is chosen to be 256. The symbols are known *a priori*. The effect of AWGN noise added by the channel is averaged out by performing approximately 100 iterations. The CFO has been chosen to be 0.18 to illustrate system performance in terms of resolution and the number of iterations required for convergence. One of the important parameters affecting the system behavior is the step size δ_{MSER}. Figure 3.9 shows the Symbol Error Rate (SER) of the system averaged over 100 trials as a function of the step size. It can be seen that at a moderate SNR of 10 dB the system performance can be improved by increasing the step size, which leads to faster convergence. If the system is operating at a higher SNR, say 16 dB, increasing the step size leads to an increased number of symbol errors. For our simulations step size in the range 0.01 to 0.02 has been used. Only for the
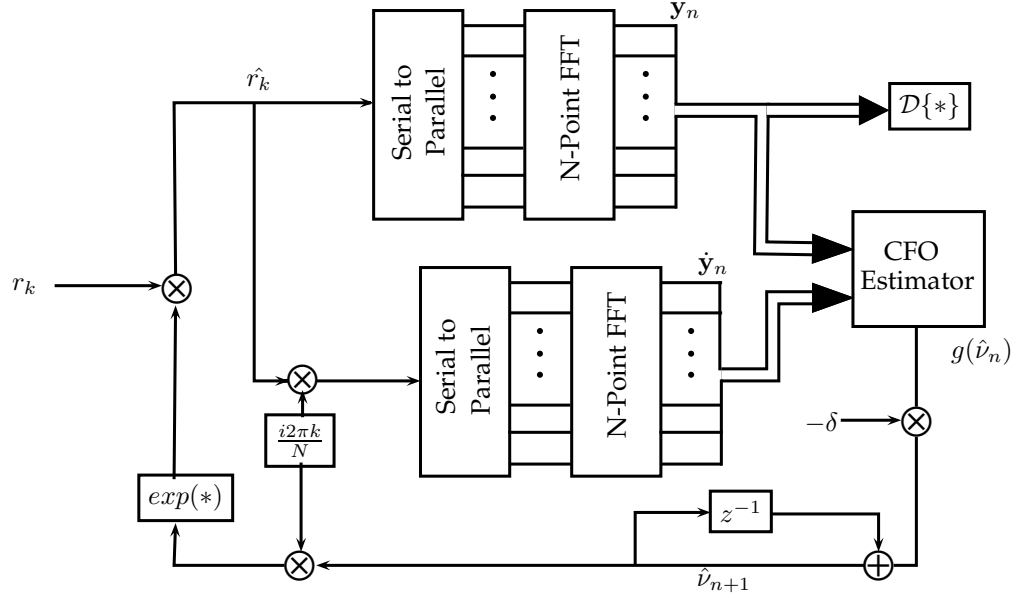
Fig. 3.8: Estimator structure. CFO estimate is updated once per OFDM block.

simulation in figure 3.9 OFDM block length of 32 has been used.

Figures 3.10-3.14 show the performance of various system parameters at SNRs of -5 dB, 0 dB, 5 dB, 10 dB, and 15 dB. The CFO estimate, Error signal, and Bit Error Rate (BER) are chosen to illustrate system performance. The number of blocks processed or the iteration number forms the time axis for these plots.

3.4.1   CFO Estimate

The number of iterations required for convergence in an iterative approach is dependent on the SNR and the step size. As mentioned in section 3.2, the MSER-based approach is particularly vulnerable to low SNR. In figure 3.10 we can observe that even after 20 iterations the CFO estimate has not converged to the true offset of 0.18. In figure 3.11 the estimator converges to the true offset in about 8 iterations. Figures 3.12 and 3.13 are the best operating regions for the MSER CFO Estimator at 5 dB and 10 dB, respectively.

In the latter case, we can observe the initial overshoot characteristic of this under-damped system. In section 3.2, it was observed that at high SNR the system is resilient to a small residual offset. In figure 3.14 at 15 dB the system does not converge to the true
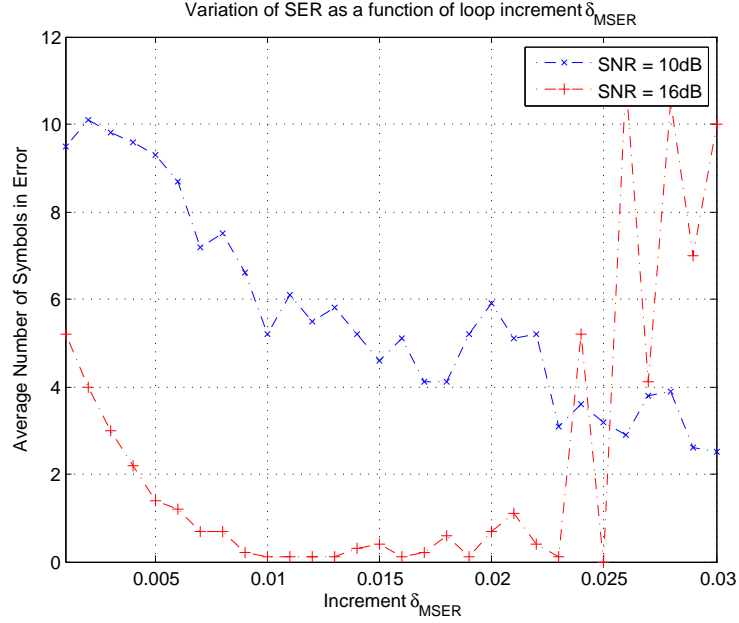
Fig. 3.9: Plot illustrating the region of operation in terms of step size δ_{MSER}.

CFO of 0.18.

3.4.2 BER Curves

Uncompensated CFO leads to Inter-Carrier Interference in OFDM systems. The recovery of transmitted symbols becomes impossible in the presence of CFO and AWGN noise added by the channel. The probability of error was analytically determined by Sathanantan and Tellambura [7] wherein it was shown that for a QPSK constellation operating at $SNR = 10 \ dB$ and $CFO = 0.2$ would perform at a Bit Error Rate of 10^{-1}. MSER focuses on minimising the BER along with the estimation of the CFO. In figure 3.13 we can see that after 5 iterations the BER drops down to 10^{-3}. This is a marked improvement over traditional CFO estimation techniques. At higher SNR of 15 dB (figure 3.14) the achievable BER of the system is approximately $10^{-4.3}$. The high initial gradient of the BER, typically in the first 3-4 iterations, seems to suggest MSER-based estimation as an alternative to other blind and data-aided equalization techniques that work on 2-5 OFDM symbol blocks.

3.4.3 Error Signal

At a low SNR of -5 dB (figure 3.10), the error signal of the MSER-CFO estimator is very small and converges to zero gradually. At higher values of SNR the error signal drops to zero typically in 3-5 iterations (figures 3.12 and 3.13). At higher values of SNR (15 dB, figure 3.14) the error signal becomes zero in 1-2 iterations. This means that the system typically never converges to the exact value of CFO. This behavior can be attributed to the approximations made with the objective function to make the gradient function easily computable. As claimed earlier (section 3.1) once sufficient number of iterations are performed the system BER drops down. However due to the high value of SNR, the argument of the Q-function is sufficiently large implying a small value of the error signal.

3.5 Comparision with ML

The Maximum Likelihood approach for CFO estimation as presented in the paper by van de Beek et al. [15] was discussed in section 2.5. It is a blind estimation technique but yet offers a good metric for comparision with MSER based CFO estimation. For our simulation OFDM block length of 256 was chosen. The system operates at a stationary CFO of 0.18. Cyclic Prefix of 32 is used in the simulation. Averaging is performed using 100 trials and a step size of 0.003 was used for the MSER approach.

For the ML approach when the time offset is unknown, the CFO can be estimated by the use of $2N + L$ receiver inputs. The computuational effort involves the calculation of average symbol correlation which can be accomplished using an accumulator. This can be contrasted with the computationally intensive error estimation in MSER. At moderate to high SNR (5-15 dB), the CFO estimate converges in about 2-3 iterations. In the following simulations, the Mean Square Error (MSE) and Bit Error Rate (BER) of the two algorithms is contrasted. For the MSER approach, we have plotted the MSE and BER curves against SNR for the three cases corresponding to 5, 3, and 2 iterations. From figure 3.15 we see that the CFO estimate for the ML approach has the lowest MSE. The BER curves, figure 3.16, for the ML approach is much better than that for the MSER approach. At SNR = 12 dB, the BER drops to $\approx 10^{-4}$ while the BER of the ML approach has a relatively high

Fig. 3.10: Plot illustrating (a - Top left) CFO estimate, (b - Top right) Error signal, and (c - Bottom) BER as a function of the iteration number at -5 dB.

Fig. 3.11: Plot illustrating (a - Top left) CFO estimate, (b - Top right) Error signal, and (c - Bottom) BER as a function of the iteration number at 0 dB.

Fig. 3.12: Plot illustrating (a - Top left) CFO estimate, (b - Top right) Error signal, and (c - Bottom) BER as a function of the iteration number at 5 dB.
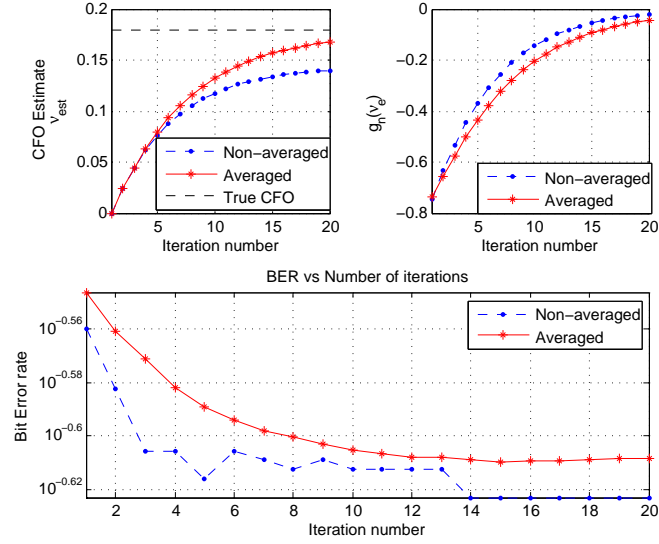

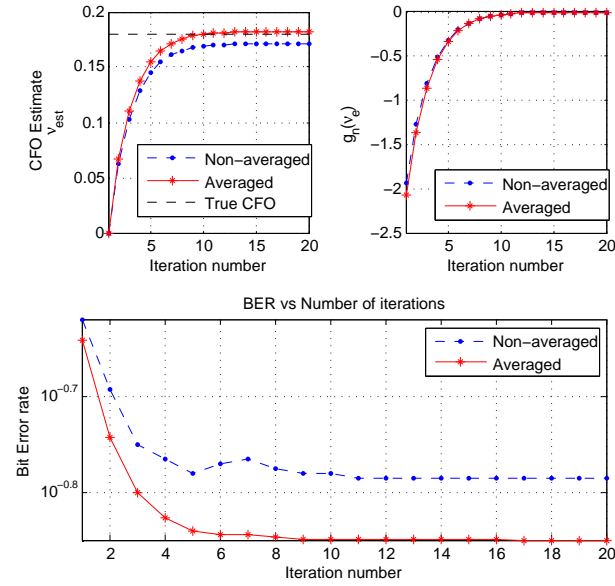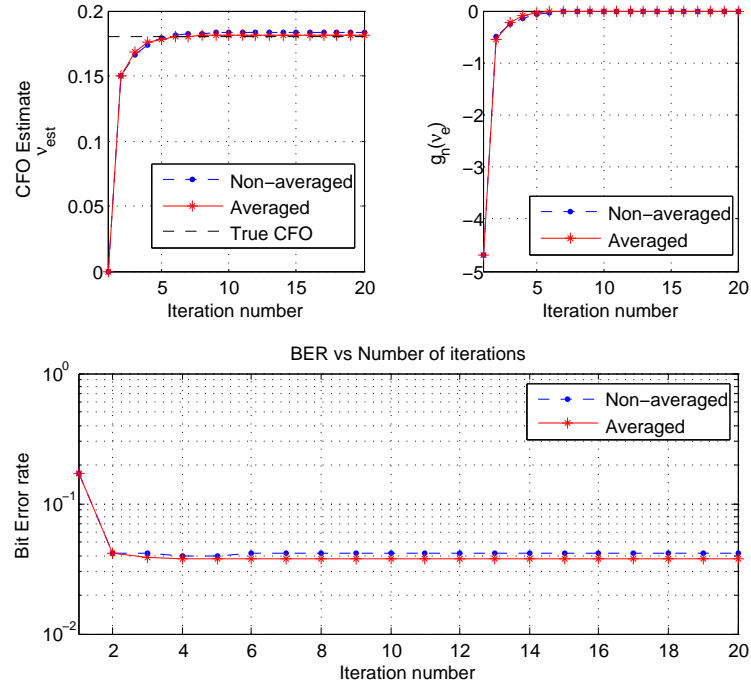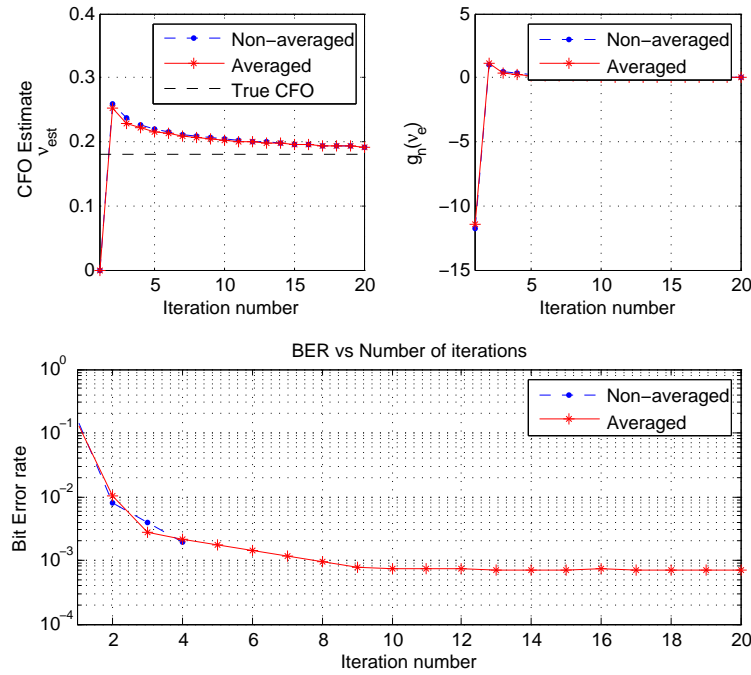
Fig. 3.13: Plot illustrating (a - Top left) CFO estimate, (b - Top right) Error signal, and (c - Bottom) BER as a function of the iteration number at 10 dB.
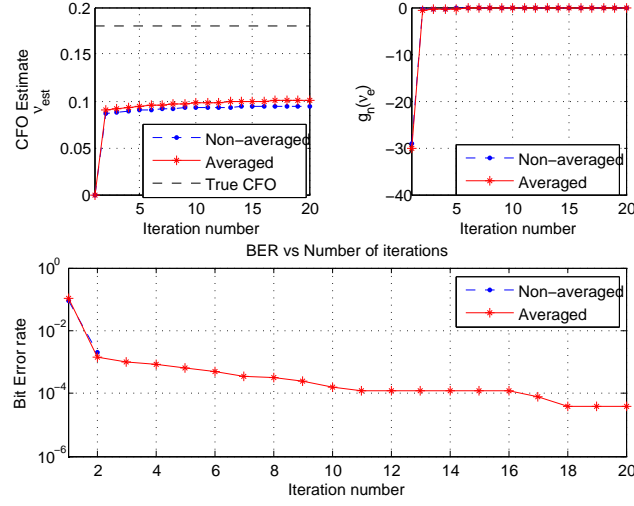
Fig. 3.14: Plot illustrating (a - Top left) CFO estimate, (b - Top right) Error signal, and (c - Bottom) BER as a function of the iteration number at 15 dB.

BER of $\approx 10^{-2}$

3.6   Improving Performance of the MSER Estimator

The performance of MSER algorithm has two major drawbacks namely, the poor performance in terms of the mean squared error of the estimate and secondly the computational complexity. This section attempts to address these issues.

3.6.1   Choice of Parameters σ and δ_{MSER}

Figure 3.9 illustrated the impact of step size δ_{MSER} on the performance of the system. It was also observed that this was a function of the signal-to-noise ratio σ. Since the expression for the error signal is dependent on σ, at high SNR the system rarely adapts over iterations. This problem can be overcome if it could be ensured that the system continiues to adapt even at higher SNR. One way this could be done is to artificially fix the value of noise variance at a predetermined value in computing the error signal. Figures 3.17 and 3.18 show the performance of the MSER system when the noise variance in equation (3.3) is held fixed at $\sigma_a = 5dB$ even while the system SNR varies independently. The performance improvement for MSER can be readily observed both in terms of the MSE and the bit error rate.
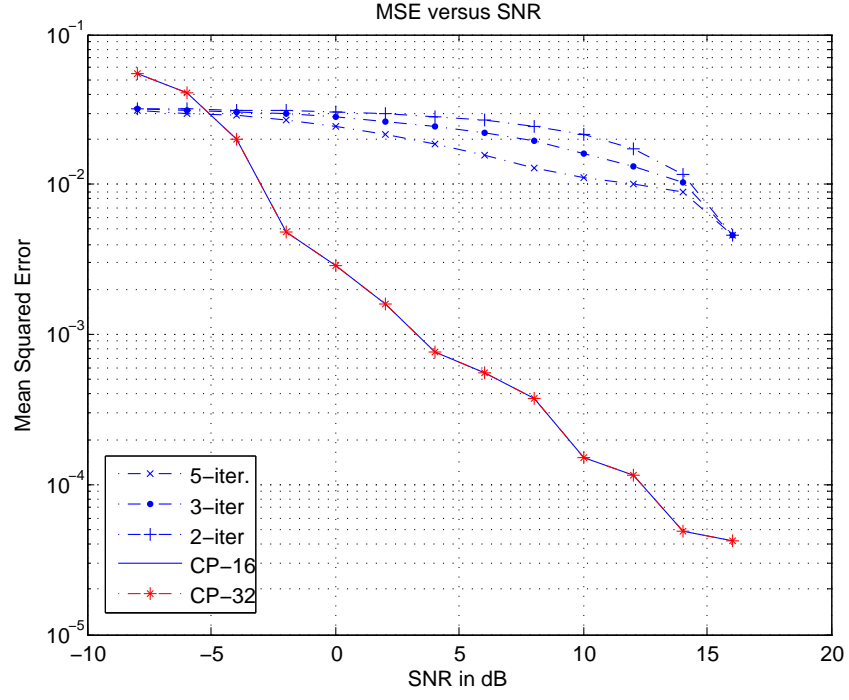
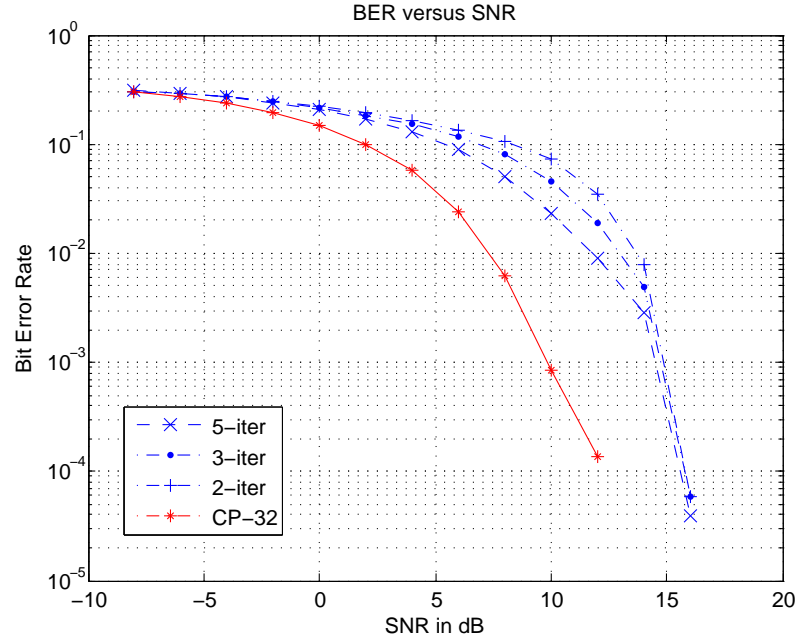Fig. 3.15: MSE of CFO estimate plotted against SNR.

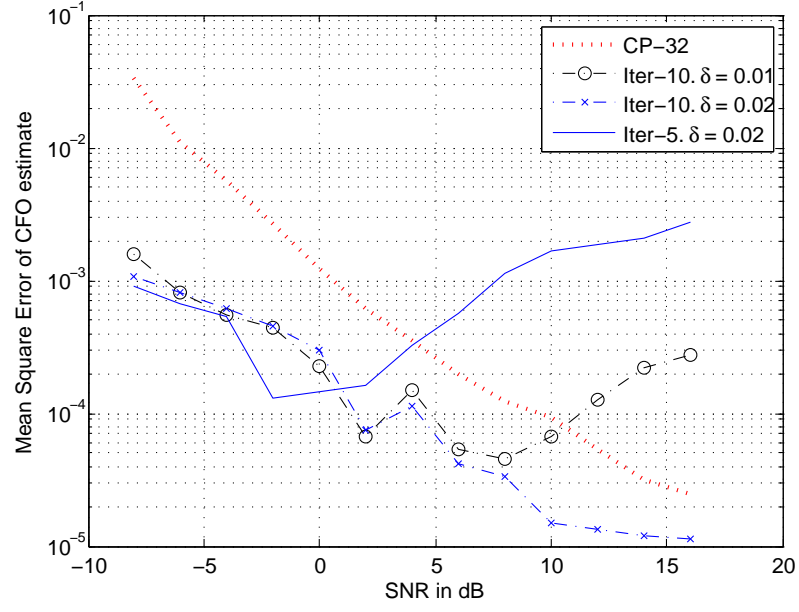Fig. 3.16: BER of the system plotted against SNR.

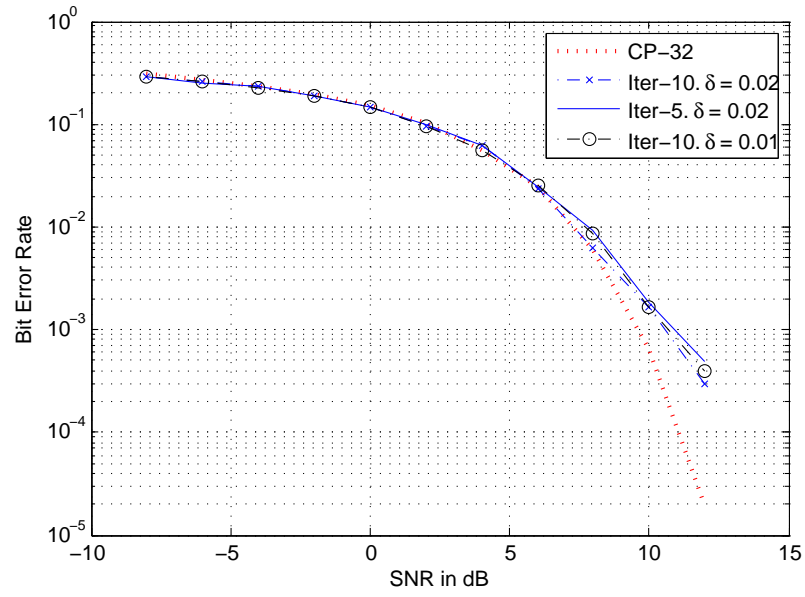Fig. 3.17: MSE of the system plotted against SNR with $\sigma_a = 5$ dB.

Fig. 3.18: BER of the system plotted against SNR with $\sigma_a = 5$ dB.

3.6.2 Derivative Based on Log-Probability

The derivative of probability of error was obtained in (3.3) using the expression for probability of error. Based on this derivative, the estimate for CFO was iteratively computed in (3.5). A similar equation can be derived by computing the log-probability of error. As shown in the Appendix B, the following function is an upper bound on the derivative of log-probability of error $\frac{\partial}{\partial \nu} \log P(e)$.

$$f(P(e), \mathbf{y}) = -E_{s_n = a_i} E_{y_n} \sum_{k=0}^{M-1} I(k \neq i) \frac{\sqrt{2} \Re((a_i - a_k)^*(\dot{y}_n))}{|a_k - a_i| \sigma} \tag{3.6}$$

This derivative can be used in the update equation and greatly reduces the computational complexity by eliminating the need to compute the value of the Q-function. Keeping the SNR fixed at 5dB in evaluating the equation (3.6), simulations as in section 3.6.1 were performed. The results are shown in figures 3.20 and 3.19.

It can be seen that the MSE performance of the log-MSER estimator has improved over the ML approach where cyclic prefixes of length 16 and 8 are used. The BER of log-MSER is slightly better than the ML based estimator.
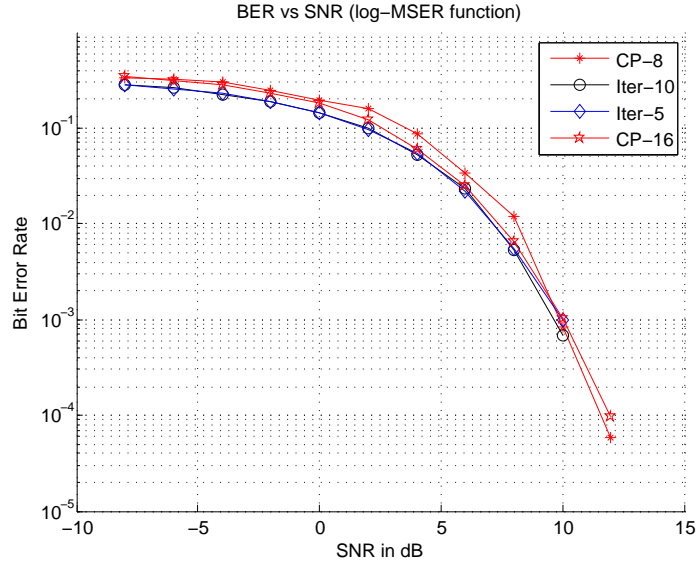

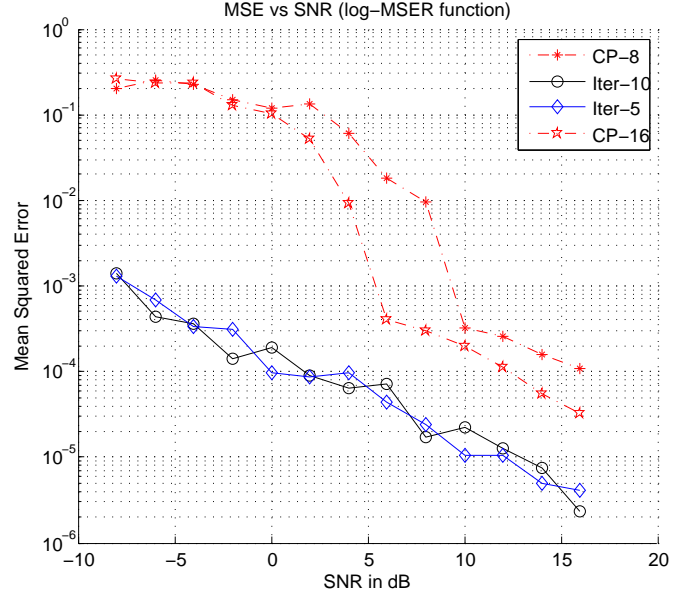Fig. 3.19: BER of the system plotted against SNR with $\sigma_a = 5$ dB. The log-MSER function is used.

Fig. 3.20: MSE of the system plotted against SNR with $\sigma_a = 5$ dB. The log-MSER function is used.

Chapter 4

Conclusions and Future Work

4.1 Conclusions

This thesis discusses the development of a carrier frequency offset estimator for OFDM using the minimum symbol error rate criterion. The development of the algorithm involved multiple phases such as formulation of the data model, obtaining a general rule for the probability of error, application of the probability of error rule for the OFDM data model. The objective of the estimator was then defined to be the minimization of the probability of symbol error under the MSER rule. This was accomplished using the gradient-descent approach and the update rule similar to the LMS algorithm [25]. The estimator update occurs once per OFDM symbol. The ML approach derived by van de Beek et al. [15] is used for benchmarking the MSER-based method. If the derivative of probability of error is used, the performance of the MSER-based estimator is found be at par with the ML approach. With a sufficient number of iterations, the MSE of the MSER-based system is can be made lower than the ML-based system, and the BER performance is comparable or only slightly worse than the ML-based system. This can be accounted due to the fact that the actual expectation in the probability of error equation is not performed. When the gradient of the log probability of error function is used in the update, the system is found to perform better than the ML-based algorithm.

Even though the use of the log-MSER function consumes lesser computuational power than the MSER-based estimator, it is more computationally intensive than the ML-based estimator. Further, the estimator provides improved performance at the cost of the number of iterations required for convergence and the requirement of pilot sysmbols. However, both of these conditions can be accomodated in the preamble-block of the communication

system. Thus, the method discussed in this thesis is suitable for burst mode of operation at high data rates wherein the tolerance for frequecy offset is very small. The ML approach described does not work well in an iterative approach and thus the estimate can not be refined further. Such a solution can be used as the initial guess of the MSER approach and the estimate may be improved by continued iterations till the desired accuracy criteria are met.

4.2   Future Work

The frequency offset estimator discussed in this thesis achieves good mean squared error performance and ensures that the OFDM system can operate with a low bit error rate at the cost of computational complexity. This system requires the transmission of pilot symbols. Further work can examine the alternative decision rules that exploit the symmetrical nature of the communication system and thereby eliminate the need for pilot symbols. The same holds true for the modified gradient function. This model only considered the AWGN channel for simulation. This work can be extended to the case of a fading channel. The performance of MSER decision rule in conjunction with convolutional codes which are a part of the OFDM implementation standards is an area for further exploration. The gradient descent method adopted in this work may be replaced by a different minimization strategy such as binary search or by an algorithm exploiting the convex nature of the probability of error.

References

[1] Z. Wang and G. Giannakis, "Wireless multicarrier communications," *IEEE Signal Processing Magazine*, vol. 17, no. 3, pp. 29–48, May 2000.

[2] S. Yang, *Orthogonal Frequency Division Multiplexed Access System Analysis and Design*. Norwood, MA; Artech House, 2010.

[3] R. Prasad, *Orthogonal Frequency Division Multiplexing for Wireless Communication Systems*. Norwood, MA; Artech House, 2004.

[4] R. W. Chang, "Synthesis of band-limited orthogonal signals for multichannel data transmission," *Bell Systems Technical Journal*, vol. 45, pp. 1775–1796, 1966.

[5] S. Weinstein and P. Ebert, "Data transmission by frequency-division multiplexing using the discrete fourier transform," *IEEE Transactions on Communications Technology*, vol. 19, no. 5, pp. 628–634, Oct. 1971.

[6] H. Schulze and C. Lueders, *Theory and Applications of Orthogonal Frequency Division Multiplexed Access and Code Division Multiplexed Access*, ch. 4. Orthogonal Frequency Division Multiplexing. Chichester, West Sussex, England; John Wiley and Sons, 2005.

[7] K. Sathananthan and C. Tellambura, "Probability of error calculation of Orthogonal Frequency Division Multiplexing systems with frequency offset," *IEEE Transactions on Communications*, vol. 49, no. 11, pp. 1884–1888, Nov. 2001.

[8] J. Armstrong, "Analysis of new and existing methods of reducing intercarrier interference due to carrier frequency offset in Orthogonal Frequency Division Multiplexing," *IEEE Transactions on Communications*, vol. 47, no. 3, pp. 365–369, Mar. 1999.

[9] Y. Zhao and S.-G. Haggman, "Intercarrier interference self-cancellation scheme for Orthogonal Frequency Division Multiplexing mobile communication systems," *IEEE Transactions on Communications*, vol. 49, no. 7, pp. 1185–1191, July 2001.

[10] C. Muschallik, "Improving an Orthogonal Frequency Division Multiplexing reception using an adaptive Nyquist windowing," *IEEE Transactions on Consumer Electronics*, vol. 42, no. 3, pp. 259–269, Aug. 1996.

[11] H. Liu and U. Tureli, "A high-efficiency carrier estimator for Orthogonal Frequency Division Multiplexing communications," *IEEE Communications Letters*, vol. 2, no. 4, pp. 104–106, Apr. 1998.

[12] T. Roman, S. Visuri, and V. Koivunen, "Blind frequency synchronization in Orthogonal Frequency Division Multiplexing via diagonality criterion," *IEEE Transactions on Signal Processing*, vol. 54, no. 8, pp. 3125–3135, Aug. 2006.

[13] U. Tureli, H. Liu, and M. Zoltowski, "Orthogonal Frequency Division Multiplexing blind carrier offset estimation: Estimation of Signal Parameters via Rotational Invariance Techniques (ESPRIT)," *IEEE Transactions on Communications*, vol. 48, no. 9, pp. 1459–1461, Sept. 2000.

[14] Y. Yao and G. Giannakis, "Blind carrier frequency offset estimation in Single Input Single Output, Multiple Input Multiple Output, and multiuser Orthogonal Frequency Division Multiplexing systems," *IEEE Transactions on Communications*, vol. 53, no. 1, pp. 173–183, Jan. 2005.

[15] J. van de Beek, M. Sandell, and P. Borjesson, "Maximum Likelihood estimation of time and frequency offset in Orthogonal Frequency Division Multiplexing systems," *IEEE Transactions on Signal Processing*, vol. 45, no. 7, pp. 1800–1805, July 1997.

[16] P. Moose, "A technique for orthogonal frequency division multiplexing frequency offset correction," *IEEE Transactions on Communications*, vol. 42, no. 10, pp. 2908–2914, Oct. 1994.

[17] T. Schmidl and D. Cox, "Robust frequency and timing synchronization for Orthogonal Frequency Division Multiplexing," *IEEE Transactions on Communications*, vol. 45, no. 12, pp. 1613–1621, Dec. 1997.

[18] M. Morelli and U. Mengali, "An improved frequency offset estimator for Orthogonal Frequency Division Multiplexing applications," *IEEE Communications Letters*, vol. 3, no. 3, pp. 75–77, Mar. 1999.

[19] J. Thomson, B. Baas, E. Cooper, J. Gilbert, G. Hsieh, P. Husted, A. Lokanathan, J. Kuskin, D. McCracken, B. McFarland, T. Meng, D. Nakahira, S. Ng, M. Rattehalli, J. Smith, R. Subramanian, L. Than, Y.-H. Wang, R. Yu, and X. Zhang, "An integrated 802.11a baseband and mac processor," in *Digest of Technical Papers, IEEE International Solid-State Circuits Conference*, vol. 2, pp. 92–415, 2002.

[20] M. Ghogho, A. Swami, and G. Giannakis, "Optimized null-subcarrier selection for Carrier Frequency Offset estimation in Orthogonal Frequency Division Multiplexing over frequency-selective fading channels," in *IEEE Global Telecommunications Conference*, vol. 1, pp. 202–206, 2001.

[21] C.-C. Yeh and J. Barry, "Adaptive minimum bit-error rate equalization for binary signaling," *IEEE Transactions on Communications*, vol. 48, no. 7, pp. 1226–1235, July 2000.

[22] C.-C. Yeh and J. Barry, "Adaptive minimum symbol-error rate equalization for quadrature-amplitude modulation," *IEEE Transactions on Signal Processing*, vol. 51, no. 12, pp. 3263–3269, Dec. 2003.

[23] J. Gunther and T. Moon, "Minimum Bayes risk adaptive linear equalizers," *IEEE Transactions on Signal Processing*, vol. 57, no. 12, pp. 4788–4799, Dec. 2009.

[24] J. Li, G. Liu, and G. Giannakis, "Carrier frequency offset estimation for orthogonal frequency division multiplexing-based wlans," *Signal Processing Letters, IEEE*, vol. 8, no. 3, pp. 80–82, Mar. 2001.

[25] T. K. Moon and W. C. Stirling, *Mathematical Methods and Algorithms for Signal Processing*, ch. 14. Prentice Hall, Englewood Cliffs, NJ, 2000 [Online]. Available: `http://www.neng.usu.edu/ece/faculty/tmoon/book/book.html`.

Appendices

Appendix A

Derivative of Probability of Error

Consider the derivative of the Q-function,

$$\frac{\partial}{\partial \nu} Q(x) = \frac{\partial}{\partial \nu} \frac{1}{\sqrt{2\pi}} \int_x^\infty \exp(-\tfrac{t^2}{2}) dt. \tag{A.1}$$

Using Leibniz' rule for differentiation under the integral sign,

$$\frac{\partial}{\partial y} \int_{a(y)}^{b(y)} f(t) dt = f(b(y)) \frac{\partial}{\partial y} b(y) - f(a(y)) \frac{\partial}{\partial y} a(y). \tag{A.2}$$

Using (A.2) in (A.1),

$$\frac{\partial}{\partial \nu} Q(x) = \frac{\partial}{\partial \nu} \frac{1}{\sqrt{2\pi}} \int_x^\infty \exp(-\tfrac{t^2}{2}) dt \tag{A.3}$$

$$= \frac{1}{\sqrt{2\pi}} \left(\exp(-\infty) - \exp(-\tfrac{x^2}{2}) \frac{\partial}{\partial \nu} x \right) \tag{A.4}$$

$$= -\frac{1}{\sqrt{2\pi}} \exp(-\tfrac{x^2}{2}) \frac{\partial}{\partial \nu} x. \tag{A.5}$$

Using the approximation that $Q(x) \approx \frac{1}{\sqrt{2\pi}} \exp(-\tfrac{x^2}{2})$,

$$\frac{\partial}{\partial \nu} Q(x) = -Q(x) \frac{\partial}{\partial \nu} x. \tag{A.6}$$

Appendix B

Approximation to the Derivative

Consider the derivative of log-probability of error,

$$\frac{\partial}{\partial \nu} \log P(e) = \frac{1}{P(e)} \frac{\partial}{\partial \nu} P(e). \tag{B.1}$$

Substituting for $P(e)$ and $\frac{\partial}{\partial \nu} P(e)$ from (2.39) and (3.3),

$$\frac{\partial}{\partial \nu} \log P(e) = \frac{-E_{y_n,\mathbf{s}} \sum_k I(k \neq i) Q\left(\frac{\sqrt{2}\Re((a_i - a_k)^*(\mathbf{h_n}^T \mathbf{s}[a_i] - \frac{a_i + a_k}{2}))}{|a_k - a_i|\sigma} \right) \frac{\sqrt{2}\Re((a_i - a_k)^*(\dot{\mathbf{h}}_n^T \mathbf{s}[a_i]))}{|a_k - a_i|\sigma}}{E_{y_n,\mathbf{s}} \sum_k I(k \neq i) Q\left(\frac{\sqrt{2}\Re((a_i - a_k)^*(\mathbf{h_n}^T \mathbf{s}[a_i] - \frac{a_i + a_k}{2}))}{|a_k - a_i|\sigma} \right)}$$

$$\tag{B.2}$$

$$= -E_{y_n,\mathbf{s}} \sum_k \frac{Q\left(\frac{\sqrt{2}\Re((a_i - a_k)^*(\mathbf{h_n}^T \mathbf{s}[a_i] - \frac{a_i + a_k}{2}))}{|a_k - a_i|\sigma} \right)}{E_{y_n,\mathbf{s}} \sum_k I(k \neq i) Q\left(\frac{\sqrt{2}\Re((a_i - a_k)^*(\mathbf{h_n}^T \mathbf{s}[a_i] - \frac{a_i + a_k}{2}))}{|a_k - a_i|\sigma} \right)}$$

$$\times I(k \neq i) \frac{\sqrt{2}\Re((a_i - a_k)^*(\dot{\mathbf{h}}_n^T \mathbf{s}[a_i]))}{|a_k - a_i|\sigma} \tag{B.3}$$

$$\leq -E_{y_n,\mathbf{s}} \sum_k I(k \neq i) \frac{\sqrt{2}\Re((a_i - a_k)^*(\dot{\mathbf{h}}_n^T \mathbf{s}[a_i]))}{|a_k - a_i|\sigma}. \tag{B.4}$$